SMC-TR-02-05

AEROSPACE REPORT NO.
TR-2000(8570)-1

Energy Content in the Stormtime Ring Current

10 March 2001

Prepared by

N. E. TURNER,[1] D. N. BAKER,[1] T. I. PULKKINEN,[2]
J. L. ROEDER,[3] J. F. FENNELL,[3] and V. K. JORDANOVA[4]

[1]University of Colorado, Boulder, CO
[2]Finnish Meteorological Institute, Helsinki, Finland
[3]The Aerospace Corp., Los Angeles, CA
[4]University of New Hampshire

Prepared for

SPACE AND MISSILE SYSTEMS CENTER
AIR FORCE MATERIEL COMMAND
2430 E. El Segundo Boulevard
Los Angeles Air Force Base, CA 90245

Engineering and Technology Group

THE AEROSPACE CORPORATION
El Segundo, California

This report was submitted by The Aerospace Corporation, El Segundo, CA 90245-4691, under Contract No. F04701-00-C-0009 with the Space and Missile Systems Center, 2430 E. El Segundo Blvd., Los Angeles Air Force Base, CA 90245. It was reviewed and approved for The Aerospace Corporation by L. T. Greenberg, Acting Principal Director, Space Science Applications Laboratory. Michael Zambrana was the project officer for the Mission-Oriented Investigation and Experimentation (MOIE) program.

This report has been reviewed by the Public Affairs Office (PAS) and is releasable to the National Technical Information Service (NTIS). At NTIS, it will be available to the general public, including foreign nationals.

This technical report has been reviewed and is approved for publication. Publication of this report does not constitute Air Force approval of the report's findings or conclusions. It is published only for the exchange and stimulation of ideas.

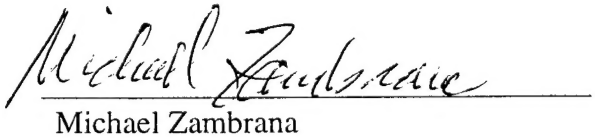

Michael Zambrana
SMC/AXE

REPORT DOCUMENTATION PAGE

Form Approved
OMB No. 0704-0188

1. AGENCY USE ONLY (*Leave blank*)	2. REPORT DATE	3. REPORT TYPE AND DATES COVERED
	10 March 2001	

4. TITLE AND SUBTITLE

Energy Content in the Stormtime Ring Current

5. FUNDING NUMBERS

F04701-00-C-0009

6. AUTHOR(S)

N. E. Turner, D. N. Baker, T. I. Pulkkinen, J. L. Roeder,
J. F. Fennell, and V. K. Jordanova

7. PERFORMING ORGANIZATION NAME(S) AND ADDRESS(ES)

The Aerospace Corporation
Laboratory Operations
El Segundo, CA 90245-4691

8. PERFORMING ORGANIZATION REPORT NUMBER

TR-2000(8570)-1

9. SPONSORING/MONITORING AGENCY NAME(S) AND ADDRESS(ES)

Space and Missile Systems Center
Air Force Materiel Command
2430 E. El Segundo Boulevard
Los Angeles Air Force Base, CA 90245

10. SPONSORING/MONITORING AGENCY REPORT NUMBER

SMC-TR-01-05

11. SUPPLEMENTARY NOTES

12a. DISTRIBUTION/AVAILABILITY STATEMENT

Approved for public release; distribution unlimited

12b. DISTRIBUTION CODE

13. ABSTRACT (*Maximum 200 words*)

Due to the important role the ring current plays in magnetospheric energetics, it is essential to understand its strength and evolution in disturbed times. There are currently three main methods for deducing the strength of the ring current: measuring ground magnetic perturbations, measuring high-altitude magnetic perturbations, or directly measuring ring current particles. The use of ground magnetometers is the most convenient, and many use the ground magnetometer-derived Dst index as a proxy for the ring current. Recent work suggests, however, that a substantial portion of Dst may not be caused only by the ring current, but also by local induction effects or other magnetospheric currents, so simply using the Dst index may yield inaccurate results. This study uses direct particle measurements to calculate the strength of the ring current and compares this to the measured Dst values. We investigate several magnetic storm intervals using the POLAR/CAMMICE experiment to measure ring current ions. We then use the Dessler-Parker-Sckopke relation to compare this to the measured Dst. This analysis is used both to understand the general behavior of the ring current compared to Dst, as well as to compare the usefulness of the Dst proxy for different types of storms. Ring current ions are shown in this analysis to contribute, on average, half of the Dst depression, with a large variety among individual events.

14. SUBJECT TERMS

Ring current, Storms, Magnetosphere, Ions

15. NUMBER OF PAGES

24

16. PRICE CODE

17. SECURITY CLASSIFICATION OF REPORT	18. SECURITY CLASSIFICATION OF THIS PAGE	19. SECURITY CLASSIFICATION OF ABSTRACT	20. LIMITATION OF ABSTRACT
UNCLASSIFIED	UNCLASSIFIED	UNCLASSIFIED	

Contents

Figures

Table

1. Introduction

Much work has been done to measure the energy in the ring current. *Hamilton et al.*, [1988], used particle measurements from the CHarge-Energy-Mass (CHEM) instrument on AMPTE/CCE to measure the energy density and evolution of the ring current for the major storm event which occurred in February of 1986. This storm lasted over a week and had a peak *Dst* value of 312 nT, which was equivalent to 368 nT when pressure corrected. They found *Dst* to be well-correlated with the inner ring current energy density from storm maximum well into recovery, but not as well-correlated during the developing main phase. The local energy density multiplied by a volume estimate, assuming azimuthal symmetry, was less than, but typically within a factor of 2 of, *Dst*. The range of measured ring current energies throughout the event was $24\% - 84\%$ of the *Dst* variation, with an average of $51.2\% \pm 17.7\%$. The peak energy content estimated was 8×10^{22} ergs, which was a factor of 14 increase from pre-storm values.

Roeder et al. [1996], studied ring current ions measured by the Combined Release and Radiation Effects Satellite (CRRES). They analyzed ions from the magnetic storm event which occurred in March of 1991. They found that ring current ions could only account for 30% *to* 50% of the *Dst* variation, and they further noted that the dusk-midnight local time position of CRRES, combined with the assumption of local time asymmetry, should overestimate the total energy.

A more statistical analysis was performed by *Greenspan and Hamilton* [2000], also using CHEM ion data from AMPTE/CCE. They studied 80 magnetic storms between

1984 and 1989 to estimate the global ring current energy. They assumed a 30% increase in *Dst* due to ground currents, and did not attempt any corrections for asymmetry, tail currents, or magnetopause currents in their data. They found a strong linear correlation between nightside ring current energy and *Dst*. Dayside measurements yielded essentially no correlation, which is suggestive of strong azimuthal asymmetry in the ring current. They found the highest ion densities in the nightside and the lowest in the morning sector, consistent with an ion population injected on the nightside which must drift and incur losses before reaching the morning sector. They calculated ratios of total ring current ion energy to *Dst* for each local time sector and found a ratio of 1.4×10^{29} keV/nT in the 6 - 12 LT sector and 2.2×10^{29} keV/nT in the 18-24 LT sector. The authors speculated that given the good agreement they found between nightside ion measurements and *Dst*, that perhaps some of the neglected effects (e.g., tail currents, magnetopause currents) might be compensatory.

Jorgensen et al. [2000], conducted a study of the global structure of the ring current using magnetic field data from CRRES. They derived an average configuration of the magnetosphere as a function of *Dst*. They sorted CRRES magnetic field data by local time and global magnetic activity (*Dst*) to produce magnetic field maps, from which they calculated local current systems. From these current maps they determined that the ring current was asymmetric for all values of *Dst*. The peak was in the afternoon sector for quiet times and near midnight during disturbed conditions. By integrating magnetic perturbations due to the ring current, the authors were able to recreate *Dst*. They found the best match when assuming a perfectly conducting Earth (which would

cause induced ground currents to increase *Dst* by 50%), and applying a 20 nT offset to *Dst*, which they interpreted as a quiet time ring current baseline.

The present study continues and improves on the earlier works by examining data from POLAR/CAMMICE and including the effects of other known current systems on *Dst*, as well as investigating and, in some cases, making corrections for ring current azimuthal asymmetry.

2. Instrumentation and Method

For this study, ion data from the Magnetospheric Ion Composition Sensor (MICS) instrument from the Charge and Mass Magnetospheric Ion Composition Experiment (CAMMICE) onboard the Polar spacecraft were used. The MICS sensor uses an ellipse-shaped electrostatic analyzer, a secondary-electron generation/detection system, and a solid-state detector to measure the energy, time-of-flight, and the energy per charge of the incident ion flux. These three parameters permit a unique determination of the ion charge state, mass, and incident energy over the energy range from 6 keV/e to 400 keV/e [*Fritz*, private communication].

The data used in this study are from March of 1996 through September of 1998. The number of passes of Polar through the ring current for different values of pressure-corrected *Dst* is shown in Figure 1.

To calculate the energy in the ring current, energy density is calculated as a function of L for each pass of the satellite. At each energy the measured local pitch angle distribution is converted to equatorial pitch angle distribution using the ratio of

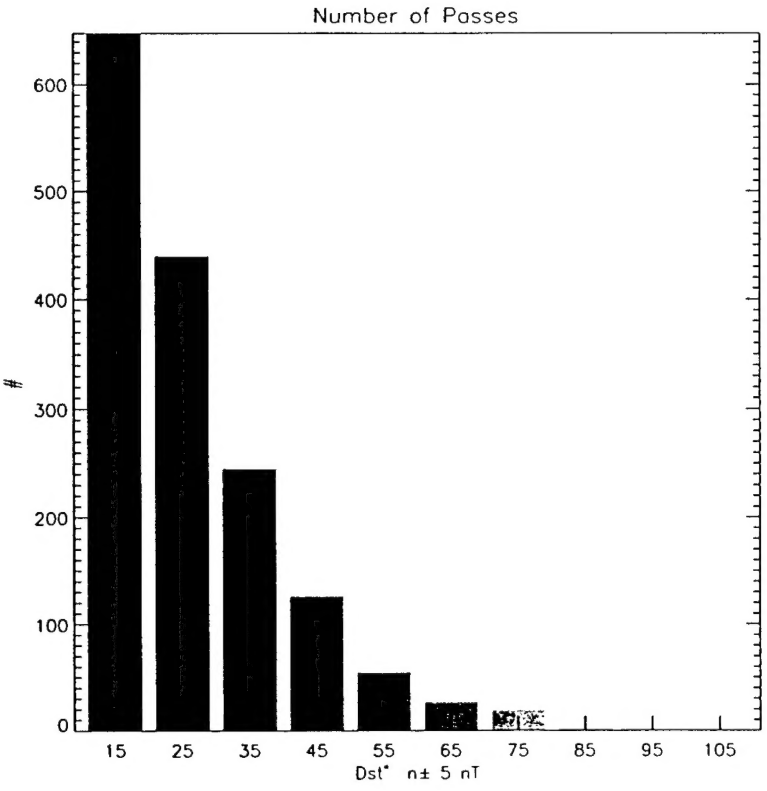

Figure 1. Number of passes of the Polar satellite through the ring current for different values of Dst^*.

measured B to the model equatorial B. The IGRF field (no external) model is used for this due to the limited activity range required for the Tsyganenko models. Once the pitch angle distribution was mapped to the equator, it is fit to $\sin^n$. The energy densities are then integrated from this equatorial spectrum [Roeder, private communication]. The energy density is then multiplied by the volume contained in each thin L-shell using Equation 1 and summed. The volume in the Earth's dipole up to a given L is calculated by

$$\text{Volume}(L) = V_E \left[L^3 \sqrt{1 - \frac{1}{L}} \left(\frac{0.43}{L^3} + \frac{0.171}{L^2} + \frac{0.229}{L} + 0.457 \right) - \sqrt{1 - \frac{1}{L}} \right] \quad (1)$$

where V_E is the volume of the Earth, 1.08×10^{21} m^3, and the resulting volume is in SI units, *Lyons and Williams* [1984, p. 8].

3. Dessler-Parker-Sckopke Relation

The standard assumption is that Dst, once corrected for the influence of other current systems, is a reliable measure of the energy content in the extraterrestrial ring current particle population. The original relationship between Dst and the energy of the ring current particles was derived by Dessler and Parker [1959] and later generalized by Sckopke [1966]:

$$\Delta B_{\text{particles}} = -\frac{\mu_0}{2\pi} \frac{W_{\text{particles}}}{B_0 R_E^3} \quad (2)$$

where $\Delta B_{\text{particles}}$ is the magnetic perturbation due to the particles, R_E is an Earth radius (6372 km), μ_0 is the permeability of free space, B_0 is the surface dipole strength at the equator, and $W_{\text{particles}}$ is the energy in the ring current particles.

4. Corrections to the *Dst* Index

When using *Dst* to estimate a physical quantity such as the ring current, it is very important to understand the physical meaning of the index. Some researchers [e.g., Campbell, 1996] have strongly cautioned about its physical derivation and interpretation. Arykov and Maltsev [1996] have argued recently that tail currents dominate *Dst* development during storms. Other researchers [e.g., Hamilton, 1988; Roeder, 1996; Kozyra et al., 1997; Jordanova et al., 1998; Greenspan and Hamilton, 2000] argue that ring current ions genuinely do significantly contribute to the *Dst* depression during storms. Given the use of *Dst* and its time variations to estimate ring current energy dissipation during storms, it is important to bracket uncertainty in the index's meaning.

4.1. Ground Current Correction

Effects due to induced currents in the ground were first discussed by *Dessler and Parker* [1959], who calculated that in a perfectly conducting planet, ground currents would enhance *Dst* by 50% and more realistic conductivity values would cause a smaller influence. Later work by *Langel and Estes* [1985] indicates that the ground currents in the Earth are proportional to 29% of the external currents at dawn and 24% at dusk, suggesting that induced currents would likely increase the magnitude of the *Dst* depression between 24% and 29%. Note that these percentages represent the fraction of the external currents, not the fraction of *Dst*. The internal and external currents are superposed in any ground magnetometer measurement. Assuming the average induced ground currents enhance *Dst* by 26.5%, removal of such an effect would require a reduction of 21% of the measured *Dst*.

4.2. Magnetopause Current Correction

Magnetopause currents have also been shown to contribute to the field perturbation felt on Earth. *Burton et al.* [1975] proposed the following formula to remove the magnetopause current contribution from the measured *Dst*:

$$Dst^* = Dst - b\sqrt{P} + c \tag{3}$$

where P is the solar wind dynamic pressure, b and c are constants, and Dst^* is the so-called pressure-corrected *Dst*.

For this study, *Burton et al.*'s equation was used for the pressure correction, with the constants b = 8.74 $\frac{\text{nT}}{\sqrt{\text{nPa}}}$, c = 11.54 nT, as calculated[1] in *O'Brien and McPherron*, [2000].

4.3. Tail Current Correction

Turner et al., [2000] describe efforts to assess the effects of the tail current system on *Dst* using the Tsyganenko [1989,1996] models. The method is to use the Tsyganenko magnetic field models to calculate the magnetic field in a GSM box-like region ($Z = \pm 5\ R_E$, $-6 > X > -50\ R_E$, and uniform in Y). The curl of the magnetic field is subsequently taken to calculate the current densities in the box. The effects of these currents are then subtracted from the data at the ground stations used for *Dst* calculations. The tail current-corrected magnetic perturbations at each of the 5 reference ground stations are then used to calculate a new *Dst*. The differences between the standard *Dst* and the tail current-corrected *Dst* were computed in each case described.

Turner et al. showed analysis for six different event intervals, which included

[1]During the revision process for O'Brien's paper, the constants have evolved very slightly. Current values are b=7.26, and c=11.0

both intense substorm events and moderate storm cases. The maximum tail current contribution was analyzed in each case versus the associated minimum *Dst* development. It was seen that there is a linear relationship between the two quantities such that the magnetotail currents account for $\sim 25\%$ of *Dst* over the modeled range of events. As noted by *Turner et al.*, it would be desirable to extend the analysis to stronger storm events, however the Tsyganenko models are not generally valid for storms with $|Dst| > 80 - 100$ nT. While some analysis was done throughout events and produced the same result, the modeling based on the most reliable data was done at the end of the growth phase for several storms. Given that this should be the time when tail currents would be most dominant, the 25% correction factor may be a slight overcorrection for other times.

4.4. Total Adjustments to *Dst*

For all events in this study, *Dst* has been pressure corrected in order to remove the effects of magnetopause currents. Additionally, the ring current energy has been scaled to an "equivalent *Dst*" by first dividing by the Dessler-Parker-Sckopke (DPS) relationship constants (see Equation 2) and then subtracting 21% for induced ground currents and another 25% for magnetotail currents. In other words, the ring current energy is scaled to 54% of the DPS-predicted *Dst* value in order to compare it with the measured (and pressure-corrected) *Dst*.

5. Ring Current Asymmetry

5.1. Asymmetry Data

The ring current is known to exhibit local time asymmetry during disturbed times. This asymmetry was studied in *Greenspan and Hamilton*, [2000], as described above. Their analysis showed the morning sector particles contributing the least to Dst and the evening sector contributing the most. Analysis with Polar data confirms this finding, as well as offers another. Figure 2 shows POLAR/CAMMICE data for all passes versus MLT. The energy from each pass is scaled to an "equivalent Dst^*" value by using Equation 2 and applying tail and ground corrections as described above, and then dividing by Dst^*. Clearly, the points on this plot range quite a bit in all local time sectors. This could be due to Polar's location (azimuthal asymmetry), magnetospheric activity level, or simply a large variety in ring current responses. Averages in each MLT sector were taken only from those points corresponding to Dst^* of less than -50 nT, not the entire data set.

To help account for the large variation evident in Figure 2, data were also sorted by magnetic activity level in addition to MLT, as shown in Figure 3. This analysis shows that the degree of measured asymmetry varies with geomagnetic activity. For each MLT sector, all available passes of POLAR data were binned according to the value of Dst^* and in each case the ring current energy was scaled to "equivalent Dst" with the DPS relation, including corrections for ground and tail currents. These values were then divided by the appropriate Dst^* value, so they show each sector's relative contribution

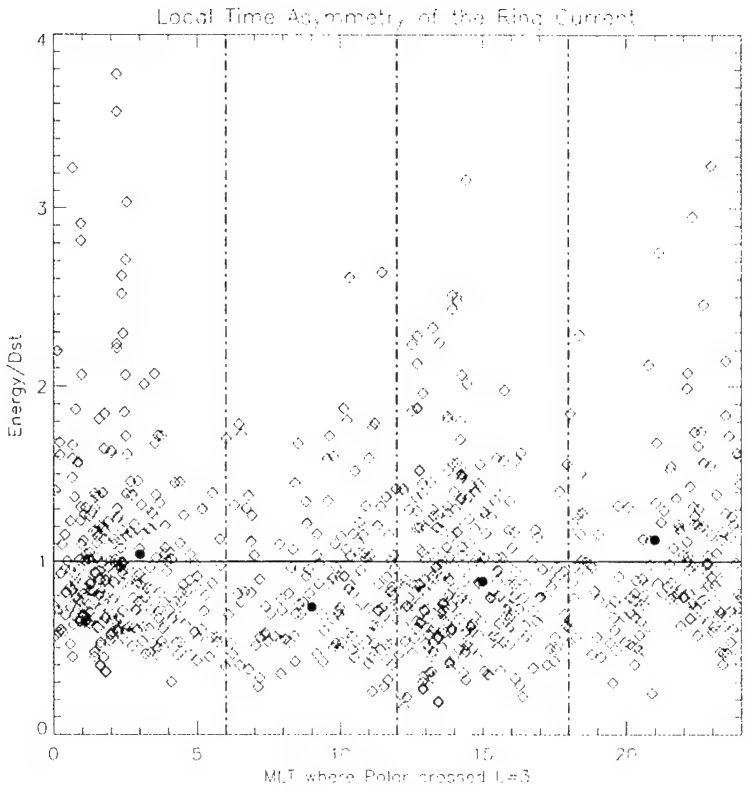

Figure 2. Ring current energy normalized by Dst^* for all events versus MLT. Red dots indicate average values shown for stormtime passes, i.e., $Dst^* < -50$ nT.

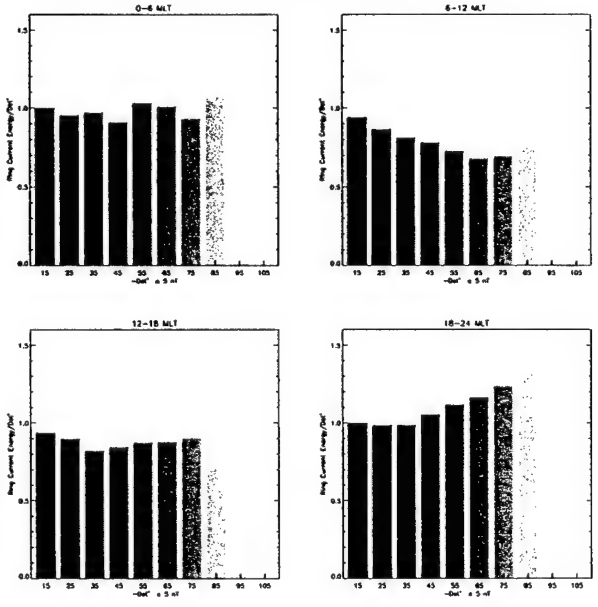

Figure 3. Ring current asymmetry is shown here as a function of Dst^*. The bars show the ratio of measured ring current energy and Dst^*, where ring current energy is scaled by the DPS relation, corrected as described in the text. Each Dst^* bin ranges 10 nT.

to *Dst*. A value close to 1 indicates an average contribution to *Dst*, while a large value indicates a disproportionately large contribution, and a value less than one corresponds to a smaller relative contribution. These data show that the evening sector becomes increasingly more important during times of large geomagnetic disturbances, while the morning and afternoon sectors become less important. This is consistent with particles being injected from the nightside rapidly during geomagnetically active times and then drifting around the Earth, incurring losses along the way. This analysis did not separate main phase versus recovery due to the limited size of the data set for periods of high activity. The late-night sector (0 - 6 MLT) seems to maintain a steadier value relative to *Dst*, which means that particle measurements in this sector correlate better with *Dst* than do measurements from other locations.

5.2. Model Correction Using Jordanova et al. Model

Figure 4 shows the pressure-corrected *Dst* index for the May 1998 storm, along with the total ring current energy for each pass of the POLAR satellite. For the purposes of comparing ring current energy with *Dst*, the ring current energy was converted into "equivalent" *Dst* by applying the DPS relation and correcting for ground and tail currents as described above. Green circles indicate dayside passes (around 10 MLT), and red circles indicate nightside passes (around 22 MLT). Panel 2 shows ring current energy values for which no asymmetry correction has been applied. For all passes in Panel 3, a model-derived asymmetry correction has been applied to help correct for the azimuthal asymmetry of the ring current. The model used was that of Jordanova et al. [1998]

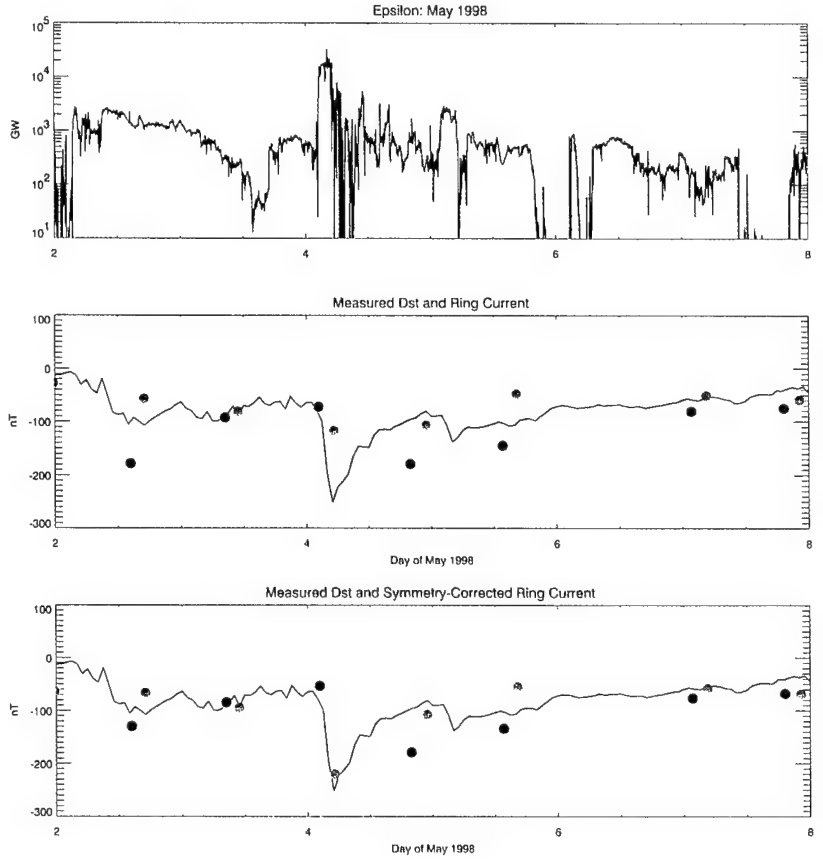

Figure 4. May, 1998 storm event. a) Epsilon, b) Dst^* and ring current energy, corrected for magnetopause, tail, and ground currents. Green circles indicate dayside passes (around 10 MLT), and red circles indicate nightside passes (around 22 MLT). c) same as (b), but also corrected for azimuthal asymmetry using Jordanova et al. model-derived correction

which follows the evolution of three major ring current ion species (H^+, He^+, and O^+) considering adiabatic drift motion and losses due to charge exchange with the hydrogen geocorona and Coulomb collisions with a time-dependent plasmasphere.

The model was used to calculate the percentage of energy density for each species as a function of time and MLT, and each POLAR data point was corrected according to these calculations. These corrected data show a very strong ring current response to the solar wind conditions. On 2 May, the ring current underwent its first intensification, corresponding to a *Dst* of around -100 nT. The second, larger intensification, followed shortly after epsilon reached 10^4 GW, and resulted in a (pressure-corrected) Dst^* value of -250 nT. The ring current energy at the peak of the storm was about 4×10^{15} J. Generally, the data show a reasonably good agreement between *Dst* and the measured ring current energy. The largest discrepancies occur in the early recovery phase, where the nightside passes are enhanced relative to the dayside passes. This indicates that the data show a stronger asymmetry than the model, and thus are not adequately corrected. For the rest of the storm, the model-corrected data appear to be consistent both with other data points from different regions, and with the pressure-corrected *Dst* index. Figure 5 shows another view of the same event. Again, the top panel is uncorrected and the bottom panel has been adjusted to account for asymmetry. The line $Y = X$ is shown to guide the eye. From this view it is clear that the largest corrections were during times of higher activity, and generally the scatter of the points is decreased from Panel a to Panel b.

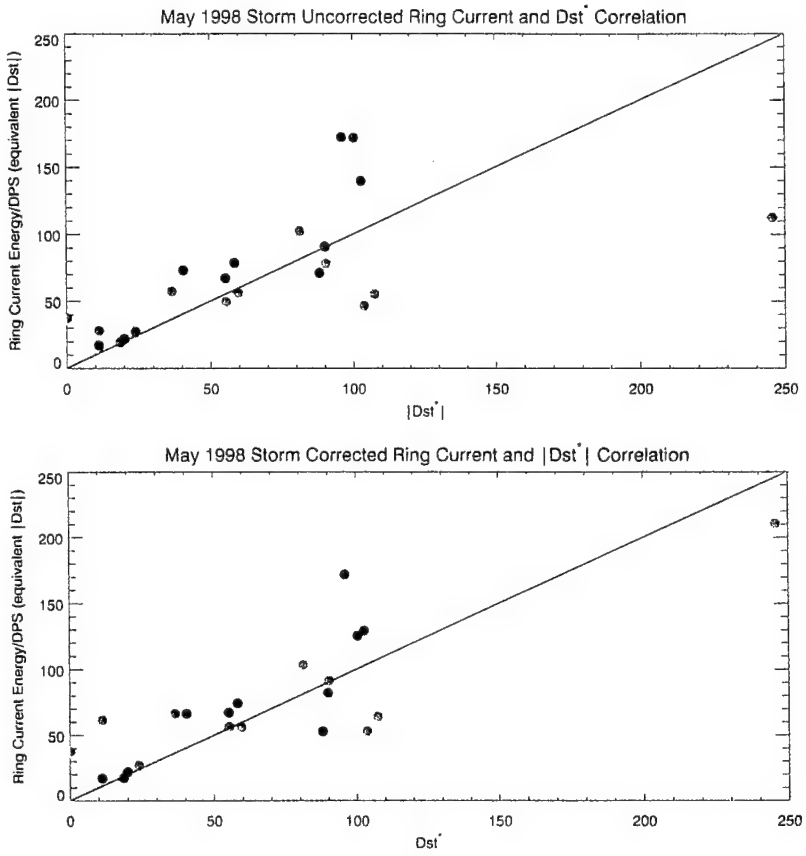

Figure 5. May, 1998 storm event: Correlations between Dst^* and measured ring current energy. Green circles indicate dayside passes (around 10 MLT), and red circles indicate nightside passes (around 22 MLT) a) Not asymmetry-corrected, b) Asymmetry-corrected.

6. Statistical Results

Statistics for all events from March of 1996 through September of 1998 are shown in Table 1. The first column shows the lower cutoff for $|Dst^*|$, followed by the percentage of Dst^* which is accounted for by ring current ions, and the standard deviation of same. Next are listed the correlations between the ring current and Dst^*: first overall, then dayside and nightside values.

Clearly, the ring current correlates more highly with Dst^* for the nightside measurements. This is likely due to the fact that the ring current is injected on the nightside and incurs losses as particles drift around the Earth. The dayside values change less over a storm and contribute less to Dst. There is also a slight trend toward higher ring current contributions to Dst during more disturbed times, which will be discussed later. Also of note is that the standard deviations of these measurements are quite large. Again, this may be due partially to ring current asymmetry, since the measurements were taken at all local times and are therefore sampling all MLT sectors. The overall correlations are high, but not overwhelming. This may also have to do with asymmetry to some extent. Additionally, the correlations get weaker as activity gets higher. This may be due to increased scatter due to the increasing asymmetry during disturbed times as well as the smaller number of data points during peak activity periods.

A scatterplot of all events in this study can be seen in Figure 6. This figure shows a moderately linear relationship between Dst and ring current energy, with scatter

Table 1. Ring Current Correlations with Dst^*

$\lvert Dst^* \rvert \geq$	Percent of Dst^*	Std. Dev.	Overall Correlation	Dayside	Nightside
20 nT	48%	±25%	.65	.57	.74
50 nT	51%	±27%	.42	.37	.56
70 nT	52%	±27%	.23	.17	.42

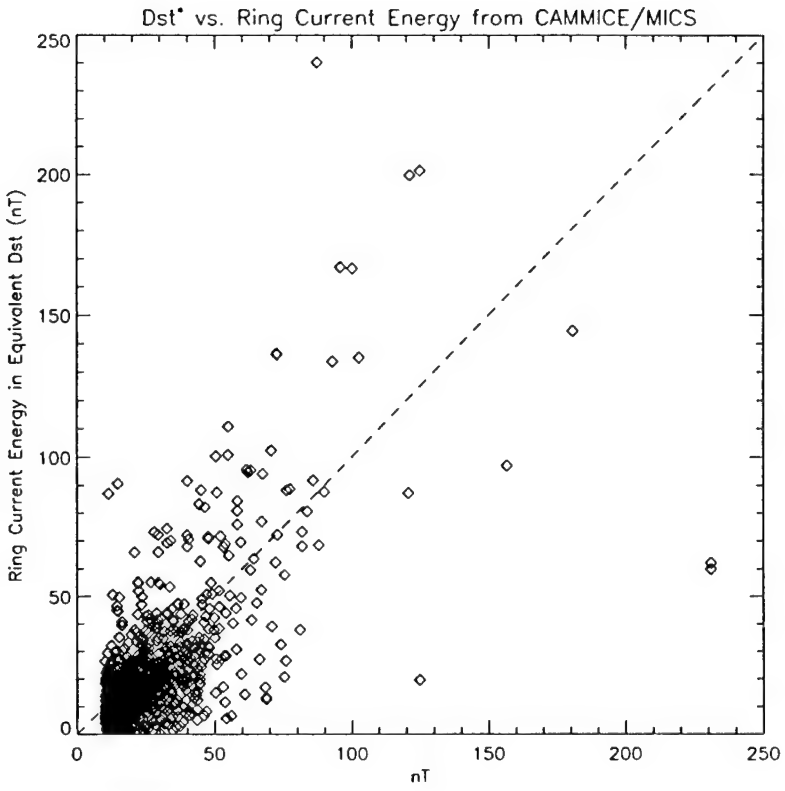

Figure 6. Correlation between $|Dst^*|$ and measured ring current energy for March 1996 through September 1998. Ring current energy is in units of equivalent Dst^*, meaning that the energy has been divided by the relevant constants in the DPS relation, including ground and tail corrections. $Y = X$ line is shown to guide the eye.

increasing as activity increases.

Figure 7 shows ring current energy in units of equivalent Dst divided by the actual Dst^* for all events. The events are binned in order to better show the behavior as a function of activity. The line $Y = 1$ shows the theoretical value: that is, it is the expected value if ground currents are 21% and tail currents are 25% of the measured Dst depression. Overall, the data fit well with the predicted values. There appears to be a trend of increasing importance of the ring current at higher activity levels. Since one of the other major contributors to Dst is the tail current system, it may be the case that the tail current is exerting a stronger influence at moderate activity levels and becomes less of a factor in very disturbed times, when the energy is transferred to the ring current. However, the number of events at high activity levels (see Figure 1) is small, so it is difficult to make strong conclusions about trends in those limited data.

7. Discussion and Conclusions

Overall, the ring current data shows surprisingly good agreement with the predicted values. The average ring current energy contributes about 50% of the measured Dst depression for most events, and slightly more during more active times, which is within statistical uncertainty of the predicted 54%. There are clear trends of increasing asymmetry and weaker energy-Dst correlations during geomagnetically active times. The nightside data do appear to correlate more highly with ground magnetometer traces than the dayside measurements. Additionally, efforts to correct for azimuthal asymmetry proved fruitful: current models do seem to handle the asymmetry well, as

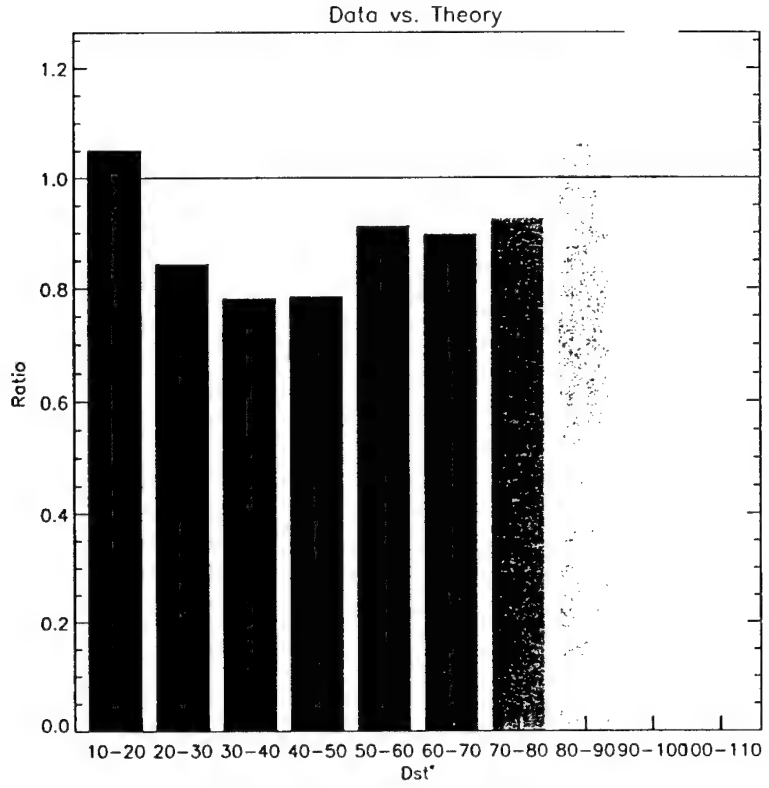

Figure 7. Relation between DPS relation data fit and Dst^* for March 1996 through September 1998. Ring current energy is converted to units of equivalent Dst^*, meaning that the energy has been divided by the relevant constants in the DPS relation, including ground and tail corrections, and then divided by Dst^*.

evidenced in the May 1998 event. Other events were not as striking as this one, since it is rare to have a Polar pass through the ring current exactly at the peak of a storm, but they did show some improvement as well.

Interestingly, while the results for these storms agreed, on average, with theoretical predictions, individual storms varied quite a lot. Certainly, some of this is due to ring current asymmetry – since most events were not asymmetry-corrected, there are many cases of over- and under-estimating the total particle energy. However, as can be seen in Figure 2, there are excursions from the theoretical values in all MLT sectors, and in both directions. It is not clear why these storms behave so differently. The standard deviations shown in Table 1 were large – around 25% – suggesting that many events did not fit this model. Studying the differences in these events, using both magnetospheric and solar wind data, might shed some light on their different dynamics.

References

Baker, D. N., N. E. Turner, and T. I. Pulkkinen, Energy transport and dissipation in the magnetosphere during geomagnetic storms, *J. Atmos. and Solar-Terrestrial Phys.*, in press, 2000.

Burton, R. K., R. L. McPherron, and C. T. Russell, An empirical relationship between interplanetary conditions and *Dst*, *J. Geophys. Res., 80*, 4204-4214, 1975.

Campbell, W. H., Geomagnetic storms, the Dst ring current myth and lognormal distributions, *J. Atmos. Solar-Terr. Phys.*, *58*, 1171-1187, 1996.

Chen, M. W., M. Schultz, and L. R. Lyons, Modeling of ring current formation and decay: a review, *Magnetic Storms*, (Eds. B. T. Tsurutani, W. D. Gonzales, Y. Kamide, and J. K. Arballo), 173-186, 1997.

Daglis, I. A., R. M. Thorne, W. Baumjohann, and S. Orsini, The terrestrial ring current: origin, formation, and decay, *Reviews of Geophys., 37*, 407-438, 1999.

Dessler A. J., and E. N. Parker, Hydromagnetic theory of magnetic storms, *J. Geophys. Res., 64*, 2239-2259, 1959.

Frank. L. A., On the extraterrestrial ring current during geomagnetic storms, *J. Geophys. Res.*, *72*, 3753-3768, 1967.

Greenspan, M. E., and D. C. Hamilton, A test of the Dessler-Parker-Sckopke relation during magnetic storms, *J. Geophys. Res.*, *105*, 5419-5430, 2000.

Hamilton, D. C., G. Gloeckler, F. M. Ipavich, W. Studemann, B. Wilken, and G.

Kremser, Ring current development during the great geomagnetic storm of February, 1986, *J. Geophys. Res., 93,* 14,343, 1988.

Jordanova, V. K., C. J. Farrugia, J. M. Quinn, R. M. Thorne, K. W. Ogilvie, R. P. Lepping, G. Lu, A. J. Lazarus, M. F. Thomsen, and R. D. Belian, Effect of wave-particle interactions on ring current evolution for January 10-11, 1997: Initial results, *Geophys. Res. Lett., 25,* 2971-2974, 1998.

Jorgensen, A. M., H. E. Spence, W. J. Hughes, and H. J. Singer, A statistical study of the global structure of the ring current, *J. Geophys. Res.*, submitted, 2000.

Kozyra, J. U., V. K. Jordanova, R. B. Horne, R. M. Thorne, Modeling of the contribution of electromagnetic cyclotron (EMIC) waves to stormtime ring current erosion, in *Magnetic Storms, Geophys. Monogr. Ser., 98,* edited by B. Tsurutani et al., p. 187, AGU, Washington, D. C., 1997.

Langel, R. A., and R. H. Estes, Large-scale, near-field magnetic fields from external sources and the corresponding induced internal field, *J. Geophys. Res., 90,* 2487-2494, 1985.

Liemohn, M. W., J. U. Kozyra, V. K. Jordanova, G. V. Khazanov, M. F. Thomsen, Analysis of early phase ring current recovery mechanisms during geomagnetic storms, *Geophys. Res. Lett., 26,* 2845-2848, 1999.

Lyons, L. R. and D. J. Williams, *Quantitative Aspects of Magnetospheric Physics,* 231 pp., D. Reidel, Hingham, MA, 1984.

O'Brien, T. P., and R. L. McPherron, An empirical phase space analysis of ring current

dynamics: Solar wind control of injection and decay, *J. Geophys. Res., 105*, 7707-7719, 2000.

Roeder, J. L., J. F. Fennell, M. W. Chen, M. Schultz, M. Grande, and S. Livi, CRRES observations of the composition of ring current populations, *Adv. Space Res., 17(10)*, 17, 1996.

Sckopke, N., A general relation between the energy of trapped particles and the disturbance field near the Earth, *J. Geophys Res. 71*, 3125, 1966.

Turner, N. E., D. N. Baker, T. I. Pulkkinen, and R. L. McPherron, Evaluation of the Tail Current Contribution to Dst, *J. Geophys. Res. 105*, 5431-5439, 2000.

LABORATORY OPERATIONS

The Aerospace Corporation functions as an "architect-engineer" for national security programs, specializing in advanced military space systems. The Corporation's Laboratory Operations supports the effective and timely development and operation of national security systems through scientific research and the application of advanced technology. Vital to the success of the Corporation is the technical staff's wide-ranging expertise and its ability to stay abreast of new technological developments and program support issues associated with rapidly evolving space systems. Contributing capabilities are provided by these individual organizations:

Electronics and Photonics Laboratory: Microelectronics, VLSI reliability, failure analysis, solid-state device physics, compound semiconductors, radiation effects, infrared and CCD detector devices, data storage and display technologies; lasers and electro-optics, solid state laser design, micro-optics, optical communications, and fiber optic sensors; atomic frequency standards, applied laser spectroscopy, laser chemistry, atmospheric propagation and beam control, LIDAR/LADAR remote sensing; solar cell and array testing and evaluation, battery electrochemistry, battery testing and evaluation.

Space Materials Laboratory: Evaluation and characterizations of new materials and processing techniques: metals, alloys, ceramics, polymers, thin films, and composites; development of advanced deposition processes; nondestructive evaluation, component failure analysis and reliability; structural mechanics, fracture mechanics, and stress corrosion; analysis and evaluation of materials at cryogenic and elevated temperatures; launch vehicle fluid mechanics, heat transfer and flight dynamics; aerothermodynamics; chemical and electric propulsion; environmental chemistry; combustion processes; space environment effects on materials, hardening and vulnerability assessment; contamination, thermal and structural control; lubrication and surface phenomena.

Space Science Applications Laboratory: Magnetospheric, auroral and cosmic ray physics, wave-particle interactions, magnetospheric plasma waves; atmospheric and ionospheric physics, density and composition of the upper atmosphere, remote sensing using atmospheric radiation; solar physics, infrared astronomy, infrared signature analysis; infrared surveillance, imaging, remote sensing, and hyperspectral imaging; effects of solar activity, magnetic storms and nuclear explosions on the Earth's atmosphere, ionosphere and magnetosphere; effects of electromagnetic and particulate radiations on space systems; space instrumentation, design fabrication and test; environmental chemistry, trace detection; atmospheric chemical reactions, atmospheric optics, light scattering, state-specific chemical reactions and radiative signatures of missile plumes.

Center for Microtechnology: Microelectromechanical systems (MEMS) for space applications; assessment of microtechnology space applications; laser micromachining; laser-surface physical and chemical interactions; micropropulsion; micro- and nanosatellite mission analysis; intelligent microinstruments for monitoring space and launch system environments.

Office of Spectral Applications: Multispectral and hyperspectral sensor development; data analysis and algorithm development; applications of multispectral and hyperspectral imagery to defense, civil space, commercial, and environmental missions.

THE AEROSPACE CORPORATION
2350 E. El Segundo Boulevard
El Segundo, California 90245-4691
U.S.A.